Electronic Supplementary Material (ESI) for Soft Matter.

SUPPORTING INFORMATION

"Molecular dynamics test of the Hertz-Knudsen equation for evaporating liquid"

R.Holyst, M.Litniewski, D.Jakubczyk

Tables, figures, and formulas given in this section are marked by numbers preceded by S. *If* S *is not present, the denotation refers to the main body of the paper.*

The factor that we take into account in simulations of gas-liquid system is the so called step error[S1] (called also the truncation error) of the numerical algorithm used for the simulation. In the case of standard Verlet algorithm[S2] applied for typical Lennard-Jones (LJ) liquid at time step $\Delta t = 0.01$ the step error "shifts" the pressure by around 0.01[S1], all in the reduced LJ units. For the LJ algorithm the "shift" is proportional to Δt^2 so the effect may be non-negligibly even for $\Delta t = 0.001$. The step error is especially important for the gas-liquid systems since the effect strongly decreases with decreasing density[S1]. As a result, even in the equilibrium state, the pressure calculated for the vapor may significantly differ from that for the liquid, which is obviously a numerical artifact due to the finite value of Δt. In our case, both for the equilibrium and non-equilibrium simulations the pressure in the gas phase was higher by around 2.5×10^{-5} from that in the liquid. Generally, the difference determines the accuracy limit for the simulation. However, here we can go beyond the limit by taking in the calculations of j_{HK} only the liquid parameters, which cancels the error in the $(p_{liq} - p_{eq})$ term in Eq(1). As a result, the ratio j_{HK}/j_m is not burdened with the discussed error. In the range of random errors, j_{HK}/j_m is constant (Fig. 2, Table S2) in spite of the fact that $(p_{liq} - p_{eq})$ changes from 2.8×10^{-5} to 1.86×10^{-4}.

In order to attain desired accuracy level, the equations of motion considered in the paper were solved applying the Cowell-Numerov[S1,S3] 4-th order implicit method:

$$\mathbf{r_i}(t+\Delta t) = 2\mathbf{r_i}(t) - \mathbf{r_i}(t-\Delta t) + \frac{\Delta t^2}{12}(\mathbf{F_i}(t+\Delta t) + 10\mathbf{F_i}(t) + \mathbf{F_i}(t-\Delta t)) \quad \text{(S1)}$$

$$\mathbf{v_i}(t+\Delta t) = \frac{\mathbf{r_i}(t+\Delta t) - \mathbf{r_i}(t)}{\Delta t} + \frac{\Delta t}{24}(7\mathbf{F_i}(t+\Delta t) + 6\mathbf{F_i}(t) - \mathbf{F_i}(t-\Delta t)) \quad \text{(S2)}$$

where $\mathbf{r}_i$, $\mathbf{v}_i$, and $\mathbf{F}_i = -\Sigma\partial\varphi_{ij}/\partial\mathbf{r}_i$ are the position, the velocity, and the force vector for the i-th particle. Eqs. (S1), were solved for the time step $\Delta t = 0.005$ using the iteration procedure from Ref. S1.

A successful analysis of simulation results requires estimation of errors. We estimated the standard error σ_e of measured quantity X by dividing the simulation data in n_d equal intervals, for 13 values of n_d varied from 8 to 20. The values of the standard deviation, σ_w , for the set of n_d data were calculated from the standard formula:

$$\sigma_w{}^2(\mathrm{X}) = \frac{1}{n_d\,(n_d-1)} \sum_{d=1}^{n_d} (<\mathrm{X}>_d - <\mathrm{X}>)^2 \qquad \text{(S3)}$$

where $<>_d$ means the average over the interval and $<>$ the average over the whole data range. were used to estimate σ_e by analyzing σ_w (S3) as a function of n_d (see also chapter 6.4 in Ref. S2). The analysis of σ_w (S3) as a function of n_d (see also chapter 6.4 in Ref. S2) was used to estimate σ_e, given in Table. S1.

n_0	L_x=L_y	L_z	T_{liq}	p_{liq}=p_{eq}	$\sigma_e(p^l_{eq})$	$(p_{liq}$-$p_{eq}(T_{liq}))/\sigma_e(p^l_{eq})$
1	91.74	704.1	0.89916(6)	0.032165(9)	0.000018	0.25
2	91.74	1008.2	0.89938(6)	0.032193(14)	0.000026	-0.68
3	90.96	943.8	0.87548(5)	0.026958(7)	0.000015	0.53
4	90.16	1009.9	0.85001(8)	0.022059(6)	0.000015	0.52
5	90.16	1468.1	0.85011(6)	0.022054(8)	0.000015	-0.96
6	88.84	1254.3	0.7971(1)	0.013966(7)	0.000013	0.08

Table S1. The results of the gas-liquid equilibrium simulations. The total time of measurements during a single simulation run amounted always to 10^5 in LJ units. The figures in parenthesis give the estimation for the standard error σ_e of the equilibrium pressure in units of the last digit of the corresponding value . T_{liq} and p_{liq}=p_{eq} are the equilibrium values for a given simulation. They were used in the minimization of Eq (6) weighted by the error in the equilibrium pressure $\sigma_e(p^l_{eq})$. Since T_{liq} and p_{liq} are not independent quantities, $\sigma_e(p^l_{eq})$ is obtained by analyzing the fluctuations of $p^i_{eq} = p^i_{liq} + (\partial p_{eq}/\partial T)_{T=T_{liq}}(T^i_{liq} - T_{liq})$ where the sup index i denotes the current value and $\partial p_{eq}/\partial T$ is taken from Eq.(6).

	L_z	$\tau/10^3$	ρ_{liq}	T_{liq}	T_{heat}	ρ_{heat}	p_{liq}	$j_m\times10^4$	$j_{HK}\times10^4$
1	1468.1	40	0.66955	0.88872	3.00	0.0100	0.02997	3.19	0.80(9)
2	1009.9	65	0.66528	0.89440	1.75	0.01825	0.03121	1.92	0.620(65)
3	1468.1	55	0.67724	0.87819	2.00	0.0140	0.02763	1.65	0.48(8)
4	1468.1	55	0.69472	0.85322	2.00	0.0115	0.02273	1.60	0.42(6)
5	1468.1	75	0.67788	0.87731	1.75	0.0160	0.02741	1.26	0.350(45)
6	1009.9	90	0.68646	0.86520	1.30	0.02025	0.02495	0.91	0.250(45)
7	1468.1	150	0.68541	0.86669	1.40	0.0188	0.02523	0.73	0.23(5)
8	1468.1	190	0.68551	0.86651	1.20	0.0225	0.02517	0.46	0.120(45)
9	1468.1	200	0.68430	0.86826	1.10	0.0255	0.02552	0.32	0.120(45)

Table S2. The evaporation parameters in the quasi stationary regime of evaporation. τ is the time of the data collection. For all systems: L_x = L_y = 90.16. The results for n_0 = 7, 8, 9 are the mean of two independent simulation runs and τ gives the sum of the times. j_{HK} is calculated during the quasi stationary stage using Eq(1) with $p_{eq}(T_{liq})$ from Eq(6). The figures in parenthesis give the standard error $\sigma_e(j_{HK})$ in units of the last digit of the corresponding value. The errors in j_m were many times

lower than $\sigma_e(j_{HK})$. For all the systems $0.85 < T_{liq} < 0.9$, during evaporation. This was the optimal range of temperature (see Table S1) for the interpolation p_{eq} by Eq(6) .

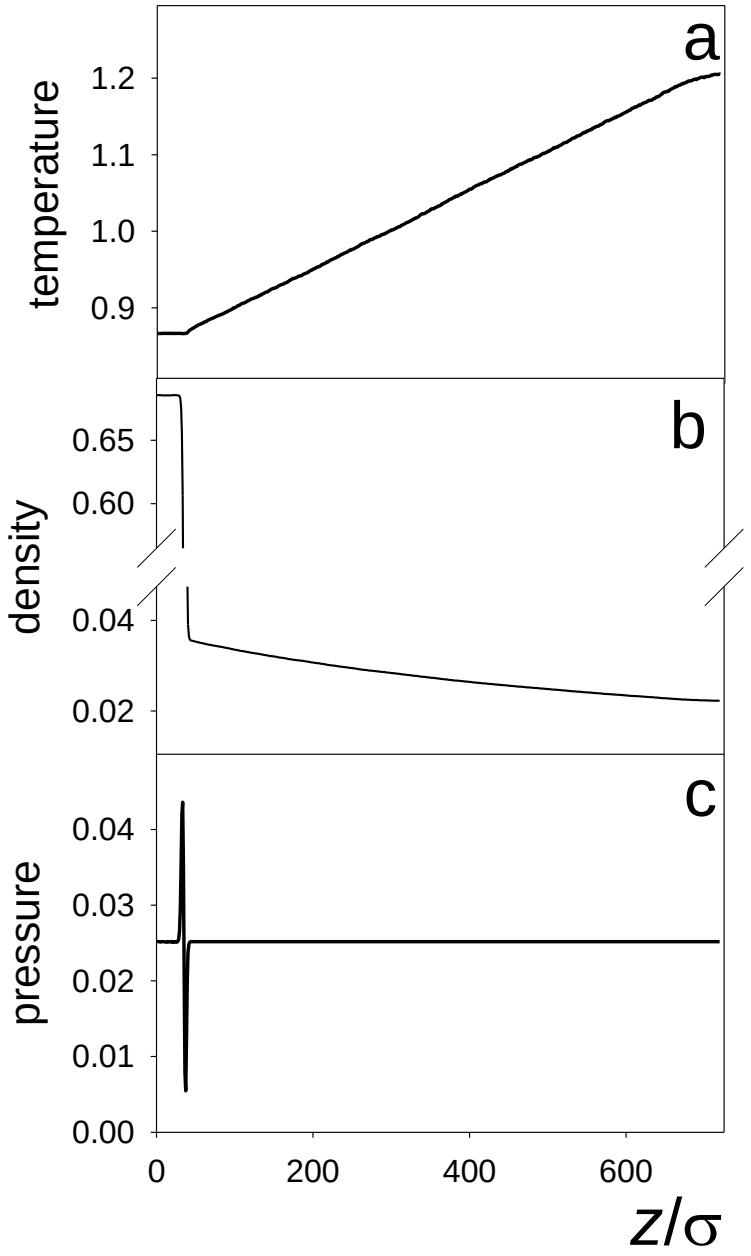

Figure S1. The profiles of the temperature (a), the density (b) and, the pressure (c) (all in the reduced LJ units) during the quasi stationary stage for the simulation run n_0 8 in Table S2. The temperature (a)

changes linearly with the distance z from T_{heat} at the border of the simulation box to T_{liq} at the gas-liquid interface. The temperature is constant and equal to $T=T_{liq}$ in the whole liquid slab. The vapor density (b) changes in such a way that together with the temperature changes assures a constant pressure in the vapor phase. Finally within the simulation error of the pressure in the liquid is equal to that in the vapor (c).

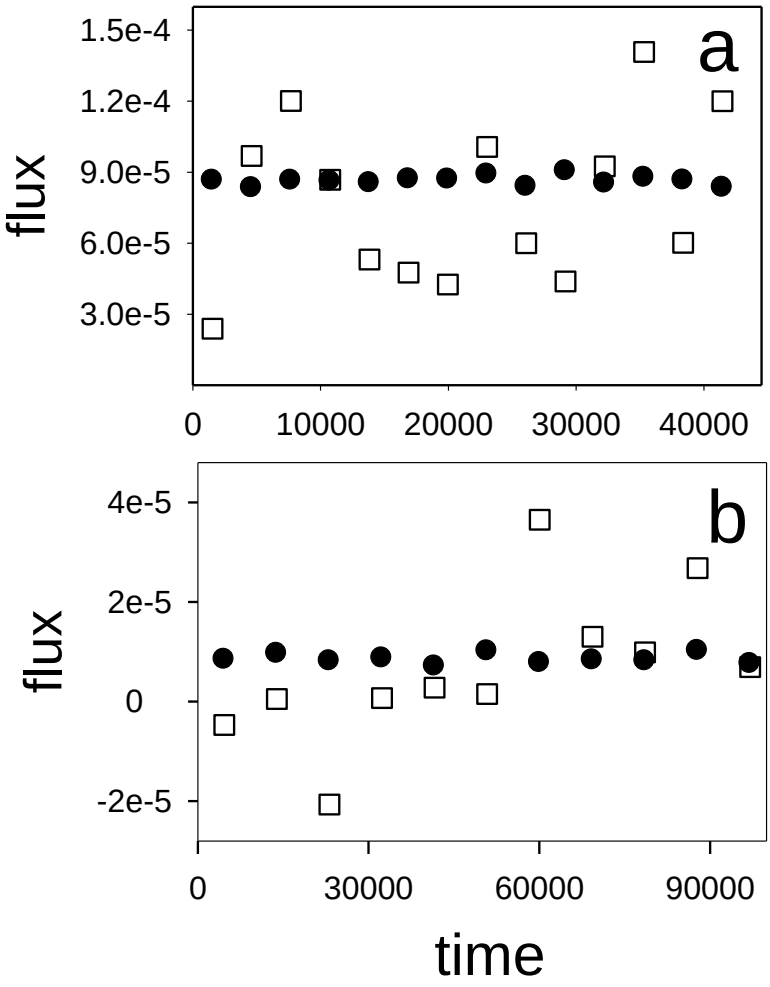

Figure S2. Current values of j_{HK} (empty squares) and $\alpha^{-1}j_m$ (black circles) as a function of time (all in the reduced LJ units) in the stationary stage for the simulation runs n_0 1 (Fig S2a) and n_0 9 (Fig. S2b) from Table S2. Both in Fig. S2a and S2b the time evolutions of of j_{HK} is characterized by very large long time fluctuations whereas j_m is nearly constant. This suggests that the mechanism of evaporation is not properly grasp by the HK equation (Eq(1)).

In the stationary regime of evaporation the flux as shown in Fig. S2 and Fig. 3 in the main textis constant. This is the main proof that our simulations are indeed in this regime. Because the evaporation is generally a very slow process therefore the differences between stationary and non-stationary regime in the density, temperature and pressure are not very pronounced. This fact is illustrated in Fig. S3 (dotted line is for non-stationary regime and red and green line are the profiles during quasi-stationary evaporation.

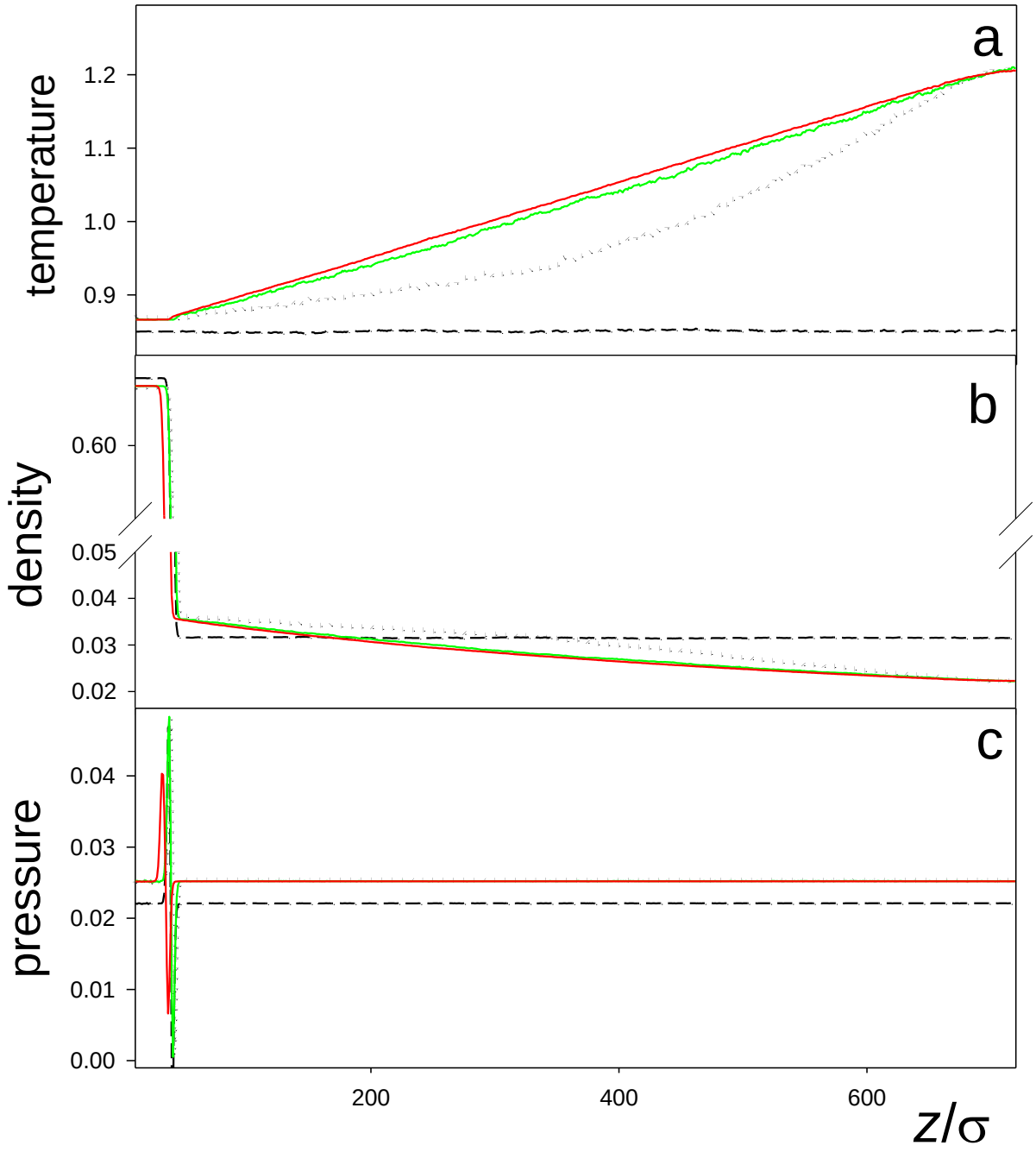

Figure S2. The temperature (a), the density (b) and the pressure (c) profile for the initial equilibrium state (the dashed line, n_0 5 in Table S1) and non-equilibrium evolutions (n_0 8 in Table S2). The dotted line represents the strongly non-equilibrium stage: the data averaged for -7000 < t < -4500. The green solid and red solid lines represent the non-equilibrium stationary stage: the data averaged for 5000 < t < 10000 (the green) and 50000 < t < 90000 (the red). t = 0 corresponds to the moment the flux j_m becomes constant. The profiles for the stationary stage are discussed in the main body of the paper.

Finally since the HK equation is based on the assumption of the Maxwell-Boltzmann velocity distribution we have tested the z-component velocity and its distribution during evaporation in the gas phase, liquid phase and in the interfacial regime. Because in LJ units the typical velocity is 1 and the average velocity in the evaporation flux is of the order of 10^{-3} the

distributions should be given by the Maxwell-Boltzmann function (MBF). Indeed Fig.S4 illustrates this hypothesis.

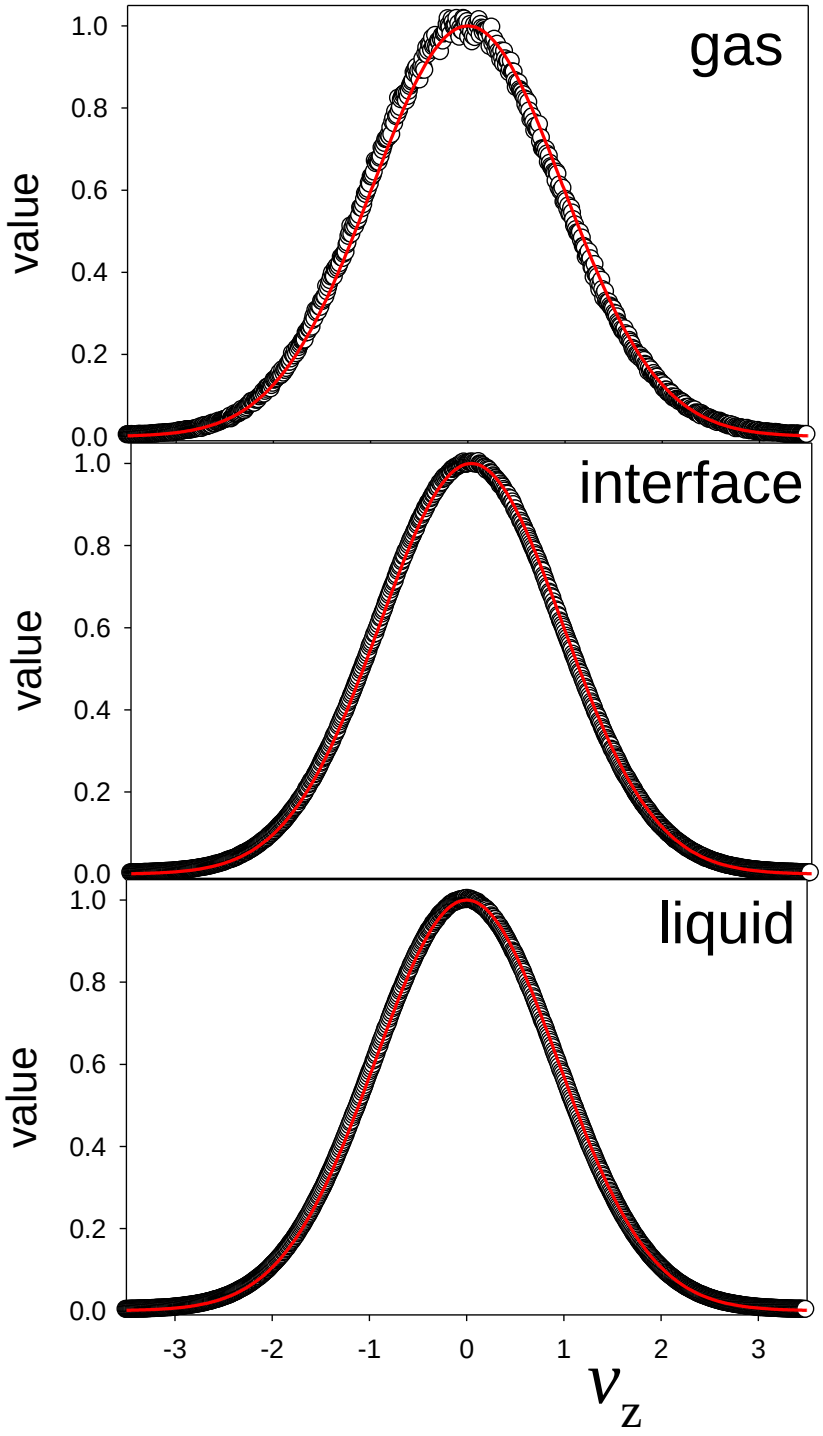

Figure S2. The velocity distribution functions (VDF(v_z), the empty circles) and the Maxwell-Boltzmann functions (MBF(v_z) = $\exp(-v_z^2/k_BT)$, the red line) for the evolution n_0 1 (Table S2). VDF(u_z) = $n_v(u_z,\Delta v_z)(2\pi k_BT)^{1/2}\Delta v_z^{-1}$ where $n_v(u, \Delta v_z)$ is the average number of particles for which $u - \Delta v_z/2 < v_z < u + \Delta v_z/2$ and $\Delta v_z = 0.01$. For the interface the data are collected from $z_{liq} - \sigma < z < z_{liq} + \sigma$ and for the gas from $z_{liq} + 18\sigma < z < z_{liq} + 22\sigma$. In all the cases VDF excellently agrees with MBF.

S1. M. Litniewski, *Mol. Simul*. **29**, 223 (2003)

S2. M. P. Allen and D. J. Tildesley, *Computer Simulations of Liquids* (Oxford University, Oxford, 1987)

S3. R. D. Skeel, G. Zhang, and T. Schlick, *SIAM J. Sci. Comput*. **18**, 203 (1997)